Monodomain dynamics for rigid rod and platelet suspensions in strongly coupled coplanar linear flow and magnetic fields

M. Gregory Forest

Department of Mathematics, Institute for Advanced Materials, Nanoscience and Technology, University of North Carolina at Chapel Hill, Chapel Hill, North Carolina 27599-3250

Qi Wang[a)]

Department of Mathematics, Florida State University, Tallahassee, Florida 32306, and School of Mathematics, Nankai University, Tianjin, 300071, People's Republic of China

Ruhai Zhou

Department of Mathematics and Statistics, Old Dominion University, Norfolk, Virginia 23529

(Received 1 February 2006; final revision received 19 October 2006)

Synopsis

Extensional flows and magnetic fields induce similar steady alignment responses when applied to liquid crystals (LCs), liquid crystal polymers (LCPs) and nematic (rigid rod or platelet) suspensions. This observation is explained for LCs by a classical analogy, expressed as a symmetry, between hydrodynamic and magnetic fields in the Leslie-Ericksen theory [de Gennes and Prost, *The Physics of Liquid Crystals* (Oxford University Press, New York, 1993); Chandrasekhar, *Liquid Crystals* (Cambridge University Press, London, 1992)]. Our purpose here is to extend this analogy: first, to LCPs and nematic suspensions where an excluded volume potential couples either to a linear flow [Hess, Z. Naturforsch. A **31a**, 1034–1037 (1976); Doi and Edwards, *The Theory of Polymer Dynamics* (Clarendon, Oxford, 1986)] or to a magnetic field [Bhandar and Wiest, J. Colloid Interface Sci. **257**, 371–382 (2003)]; and second, to the strong coupling of excluded volume interactions, planar linear flows, and a coplanar magnetic field. The general symmetries reveal parameter redundancies in the Doi-Hess kinetic theory, leading to a reduced model with significant computational savings. That is, a rotational planar linear LCP (or nematic suspension) flow under an imposed coplanar magnetic field is reducible to a simple shear flow coupled with a transversely imposed magnetic field and negative anisotropy through an orthogonal transformation; whereas a magnetic field coupled linear, irrotational flow corresponds to a tri-directional elongation. We illustrate these results with a second-moment tensor model to predict how a variable strength, coplanar magnetic field may be used to alter or control flow-induced responses of LCPs or nematic suspensions. The illustrations are for sheared dynamic attractors

[a)]Author to whom correspondence should be addressed; electronic mail: wang@math.fsu.edu

PROOF COPY 006701JOR

(tumbling, kayaking and chaotic), extension-induced steady states, and four roll mill flows.
 [DOI: 10.1122/1.2400704]

I. INTRODUCTION

Imposed magnetic fields often induce magnetic moments on rod or platelet particles in suspension, which may be exploited to control the orientation of liquid crystals, liquid crystal polymers, and anisotropic colloidal suspensions. Likewise, flow-induced torques achieve similar responses. For small molecule liquid crystals, it is well known that extensional flows and magnetic fields yield equivalent responses, a classical analogy which is described by a symmetry of the Leslie-Ericksen (L-E) director theory [de Gennes and Prost (1993); Chandrasekhar (1992)].

Liquid crystal polymers (LCPs) consist of rigid rod or platelet macromolecules of finite aspect ratio in a viscous solvent, for which nonlocal excluded volume interactions are important in understanding their behavior at rest (e.g., the isotropic-nematic phase transition) and in response to additional applied fields. The L-E director theory has been generalized to describe LCPs, with Landau-deGennes second-moment tensor models and with the Doi [Doi and Edwards (1986)] and Hess (1976) kinetic theory for the orientational probability distribution of the rod or platelet ensemble. The tensor models all can be recovered from the kinetic theory by appropriate closure rules (cf. [Forest and Wang (2003)]). Not surprisingly, LCP models display a richer class of symmetries when linear flow fields and a magnetic field are coupled with an excluded volume potential. Several of these symmetries have been noted previously for the Doi-Hess kinetic theory and its second-moment tensor approximations. Our purpose in this paper is to combine these observations into a more general class of symmetries for nematic polymers (LCPs) where an excluded volume potential is strongly coupled to coplanar linear flow and magnetic fields. This result identifies a reduced model, with three less parameters than the full model, which is amenable to existing numerical codes. We then illustrate utility of this generalized analogy by computing monodomain response diagrams versus magnetic field strength for several types of flow fields.

II. MATHEMATICAL FORMULATION

The theoretical framework of this paper is the Doi-Hess kinetic theory for linear flows of rigid spheroids immersed in a viscous solvent [Isihara (1951); Hess (1976); Kuzuu and Doi (1983); Wang (2002)]. This is a mean-field theory for nematic (or liquid crystalline) polymers and rigid rod or platelet suspensions whose equilibrium phases are governed by excluded volume interactions. A general potential has the form

$$V_i(\mathbf{m},\mathbf{x},t) = \nu kT \int_{\|\mathbf{m}'\|=1} B(\mathbf{m},\mathbf{m}') f(\mathbf{m}',\mathbf{x},t) d\mathbf{m}', \tag{1}$$

where ν is the number density of spheroids per unit volume, $\mathbf{m}$ and $\mathbf{m}'$ are axes of symmetry of respective spheroids, $B(\mathbf{m},\mathbf{m}')$ is the excluded volume [Isihara (1951)] and f is the orientational probability density function (PDF) of the ensemble of spheroids. We consider nematic liquids for which an imposed magnetic field induces a magnetic moment; intrinsic magnetic moments and magnetic dipole-dipole interactions are presumed negligible (nonferromagnetic spheroids). For such systems, the potential due to the external field is given by [Doi and Edwards (1986); de Gennes and Prost (1993); Bhandar and Wiest (2003)]

$$V_H = -\frac{\chi_\alpha}{2}(\mathbf{H}\cdot\mathbf{m})^2, \tag{2}$$

where $\mathbf{H}$ is the magnetic field vector, and χ_α (normally positive for paramagnetic materials and negative for diamagnetic materials) is the difference between the susceptibility parallel and perpendicular to the spheroid axis, also known as the magnetic anisotropy.

The rotational transport equation for the orientational probability distribution function (PDF) is given by the Smoluchowski equation [Doi and Edwards (1986); Hess (1976); Bhandar and Wiest (2003)]:

$$\frac{\partial f}{\partial t} = \mathcal{R}\cdot\left[D_r(a) f \mathcal{R}\left(\mu + \frac{1}{kT}V_H\right)\right] - \mathcal{R}\cdot[\mathbf{m}\times\dot{\mathbf{m}} f],$$

$$\dot{\mathbf{m}} = \mathbf{W}\cdot\mathbf{m} + a[\mathbf{D}\cdot\mathbf{m} - \mathbf{D}{:}\mathbf{mmm}], \tag{3}$$

where $D_r(a)$ is the rotational diffusivity (assumed to be constant in this study); $\mathcal{R}=\mathbf{m}\times\partial/\partial\mathbf{m}$ is the rotational gradient operator; $\mathbf{D}$ and $\mathbf{W}$ are the rate-of-strain and vorticity tensor, respectively; a is a geometry or shape parameter defined by $a=r^2-1/r^2+1$ where r is the spheroid aspect ratio; and $\mu=\ln f+(1/kT)V_i$ is the normalized chemical potential. We remark that the assumption on D_r to be constant, depending only on the geometry parameter of the spheroid, only affects the orientational dynamics quantitatively [Larson and Öttinger (1991)]; in our experience, nonessential details of individual orbits of the Smoluchowski equation are affected, but not the stable solutions which are the focus of this study.

We note that

$$\mathcal{R}V_H = -\chi_\alpha \mathbf{m}\times\mathbf{HH}\cdot\mathbf{m}. \tag{4}$$

With this, Eq. (3) can be rewritten as

$$\frac{df}{dt} = \mathcal{R}\cdot[D_r(a) f\mathcal{R}\mu] - \mathcal{R}\cdot[\mathbf{m}\times(\dot{\mathbf{m}} + \chi\mathbf{HH}\cdot\mathbf{m})f], \tag{5}$$

where $\chi=D_r\chi_\alpha/kT$ is a normalized magnetic anisotropy. This formulation shows the standard Jeffery orbit [Jeffery (1922)] $\dot{\mathbf{m}}$ (3) due to macroscopic flow is modified by an additional transport due to magnetic forcing. For purposes of extracting a generalized symmetry, we now modify this coupled flow-magnetic field transport term, making use of $\mathbf{m}\times\mathbf{m}=0$:

$$\mathbf{m}\times(\dot{\mathbf{m}} + \chi\mathbf{HH}\cdot\mathbf{m}) = \mathbf{m}\times\left\{\mathbf{W}\cdot\mathbf{m} + \left[a\mathbf{D} + \chi\left(\mathbf{HH} - \frac{H^2}{k}\mathbf{I}\right)\right]\cdot\mathbf{m} - \left[a\mathbf{D} + \chi\left(\mathbf{HH} - \frac{H^2}{\ell}\mathbf{I}\right)\right]{:}\mathbf{mmm}\right\}, \tag{6}$$

where k, ℓ can be any nonzero numbers and $H=\|\mathbf{H}\|$.

Recall the Smoluchowski equation absent of external fields is invariant under orthogonal transformations, which reflects orientational degeneracy of ordered equilibria f_{eq} due to excluded volume interactions. If $\mathbf{n}=\mathbf{U}\cdot\mathbf{m}$, where $\mathbf{U}$ is an orthogonal matrix, then Eq. (5) leads to

$$\frac{d\tilde{f}}{dt} = \mathcal{R}_n \cdot [D_r(a)\tilde{f}\mathcal{R}_n\tilde{\mu}] - \mathcal{R}_n \cdot [\mathbf{n} \times (\dot{\mathbf{n}} + \chi\tilde{\mathbf{H}}\tilde{\mathbf{H}} \cdot \mathbf{n})\tilde{f}], \tag{7}$$

where the PDF $\tilde{f}=\tilde{f}(\mathbf{n},\mathbf{x},t)=f(\mathbf{U}^T\cdot\mathbf{n},\mathbf{x},t)$, $\mathcal{R}_n=\mathbf{n}\times\partial/\partial\mathbf{n}$, $\tilde{\mathbf{H}}=\mathbf{U}\cdot\mathbf{H}$ is the rotated external field, and $\tilde{\mu}=\ln\tilde{f}+(1/kT)V_i(\mathbf{n},\mathbf{x},t)$. So, if $\mathbf{U}\cdot\mathbf{H}=\mathbf{H}$, the invariance retains under a reduced symmetry, i.e., it is invariant under the rotational subgroup $SU(2,\mathbf{H})=\{\mathbf{U}|\mathbf{U}\cdot\mathbf{H}=\mathbf{H},\mathbf{U}\in SU(3)\}$. We pause now to establish the classical analogy of small molecule liquid crystals from this formulation.

III. CLASSICAL MAGNETIC FIELD AND EXTENSIONAL FLOW ANALOGY

We assume there is only a constant magnetic field $\mathbf{H}$ and a constant flow field ($\mathbf{v}=\mathbf{v}_0$). The tensor $\mathbf{HH}$ has rank one, so there exists an orthogonal matrix $\mathbf{U}_0$ such that

$$\mathbf{HH} = \mathbf{U}_0^T \cdot \mathrm{diag}(H^2,0,0) \cdot \mathbf{U}_0. \tag{8}$$

The constant flow field exerts zero flow gradient, i.e., $\mathbf{W}=\mathbf{D}=0$. We choose $k=l=3$ in (6). Then, the Jeffery orbit becomes

$$\mathbf{m} \times (\dot{\mathbf{m}} + \chi\mathbf{HH} \cdot \mathbf{m}) = \mathbf{m} \times \chi[\mathbf{D}_e \cdot \mathbf{m} - \mathbf{D}_e\mathbf{:mmm}], \tag{9}$$

where $\chi\mathbf{D}_e=\chi(\mathbf{HH}-(H^2/3)\mathbf{I})$ is a second order, trace-free tensor which can be viewed as an effective rate-of-strain tensor. In rotated coordinates $\mathbf{n}=\mathbf{U}_0\cdot\mathbf{m}$, the Jeffery orbit is

$$\mathbf{n} \times (\dot{\mathbf{n}} + \chi\tilde{\mathbf{H}}\tilde{\mathbf{H}} \cdot \mathbf{n}) = \mathbf{n} \times [\mathbf{D}_H \cdot \mathbf{n} - \mathbf{D}_H\mathbf{:nnn}], \tag{10}$$

where $\mathbf{D}_H=\chi\mathrm{diag}(2H^2/3,-H^2/3,-H^2/3)$ is the rate-of-strain tensor for an effective pure extensional flow field with extension rate $(2/3)H^2$ and $\tilde{\mathbf{H}}=\mathbf{U}_0\cdot\mathbf{H}$ is the rotated magnetic field. The effective extensional flow is uniaxial (biaxial) extension if the anisotropy χ is positive (negative). Thus, a constant amplitude and directional magnetic field coupled to the Smoluchowski equation of Doi and Hess is equivalent to a pure extensional flow applied to LCPs.

One may now appeal to results on pure uniaxial and biaxial extension of rod-like and platelet suspensions with an excluded volume potential [Rey (1995a); Rey (1995b); Wang (1997); Forest *et al.* (2000a, 2000b); Wang *et al.* (2005)], and immediately infer complete response diagrams versus strength of an applied DC magnetic field. The latter reference is for the PDF of kinetic theory, while the others were restricted to second-moment closure models of Landau-deGennes type. Thus, this symmetry confirms well-known experimental phenomena: steady orientational distributions emerge under an imposed magnetic field, with a unique stable direction of orientation of the PDF aligned with the applied magnetic field. For $\chi>0$, uniaxial steady states are predicted, while biaxial states are predicted for $\chi<0$. The only variability due to volume fraction, field strength, and particle geometry is in the details (degree of focusing about the peak axis, as determined from the order parameters) of the PDF. This establishes the equivalent result of L-E director theory of liquid crystals or the Landau-deGennes tensor model and Doi-Hess Smoluchowski equation for LCPs and rigid rod suspensions.

Remark: Equilibria of the Smoluchowski equation subject to an imposed external potential field is of Boltzmann or Maxwell type (cf. [Onsager (1949); Constantin and Vudadinovic (2005)]. In a recent paper by one of the authors [Wang *et al.* (2005)], it is proven that all steady state solutions of the Smoluchowski equation are given by the Boltzmann-type distribution, parametrized by a pair of order parameters; the solutions and their stability can then be inferred by solving a nonlinear algebraic-integral equation system and examining the system's free energy density. The symmetry presented here, coupled with this recent theorem, establishes the same conclusions for irrotational flows and magnetic fields applied to nematic polymers, for general kinetic models of Doi-Hess type [Forest *et al.* (2006)]. Extensions to more general intermolecular potentials are given in Gopinath *et al.* (2005).

IV. GENERALIZED ANALOGY FOR COUPLED COPLANAR FLOWS AND MAGNETIC FIELDS

If we now consider Eq. (6) with nonzero $\mathbf{W}$ and $\mathbf{D}$, the same analysis presented above absorbs the magnetic field into an effective velocity field of an incompressible fluid with vorticity tensor $\mathbf{W}$ and rate-of-strain tensor $a\mathbf{D}+\chi(\mathbf{HH}-(H^2/k)\mathbf{I})$ with $k=\ell=3$. The magnetic field is equivalent to a pure elongational flow component in the direction of $\mathbf{H}$. Thus, the trade-off noted above still applies if there is an arbitrary linear flow coupled with either the magnetic field or a pure extensional flow.

We recall that the Doi-Hess kinetic model and associated second-moment tensor models for linear planar flows of LCPs obey a purely hydrodynamic correspondence principle [Forest *et al.* (2004a, 2004b)]. Rather than a "one for one" trade-off in parameters as in the classical symmetry between extensional flow and a magnetic field, the hydrodynamic symmetry reduces the number of model parameters. Our goal now is to combine these two observations into a generalized symmetry, which applies to the full coupling of excluded volume, a linear planar flow, and a coplanar magnetic field. The reduction in model parameters turns out to be quite significant, from six to three, and fortuitously, the reduced model requires only a simple modification of our existing numerical codes. In the last section, we solve the reduced model to illustrate predictions gained by application of this generalized symmetry.

Consider a linear planar flow field

$$\mathbf{v}=(v_{11}x+v_{12}y,v_{21}x-v_{11}y,0) \tag{11}$$

where v_{ij} are constants, with gradient

$$\nabla\mathbf{v}=\begin{pmatrix} v_{11} & v_{12} & 0\\ v_{21} & -v_{11} & 0\\ 0 & 0 & 0\end{pmatrix} \tag{12}$$

and a coplanar magnetic field $\mathbf{H}=(H_1,H_2,0)^T$. Let

$$p=\frac{1}{2}(v_{12}+v_{21}),\quad q=\frac{1}{2}(v_{12}-v_{21}). \tag{13}$$

We first consider $q\neq 0$ corresponding to a flow field with nonvanishing rotational component. We choose $k=\ell=2$ in Eq. (6) so that the upper left 2×2 submatrix of $a\mathbf{D}+\chi(\mathbf{HH}-(H^2/2)\mathbf{I})$ is traceless. This 2×2 submatrix qualifies as an effective rate-of-strain tensor. Then, $\mathbf{W}=q\mathbf{W}_0$ and

$$a\mathbf{D}+\chi\mathbf{HH}-\frac{\chi H^2}{2}(\mathbf{e}_1\mathbf{e}_1+\mathbf{e}_2\mathbf{e}_2+\mathbf{e}_3\mathbf{e}_3)=\lambda\mathbf{U}^T\cdot\mathbf{D}_0\cdot\mathbf{U}-\frac{\chi H^2}{2}\mathbf{e}_3\mathbf{e}_3, \tag{14}$$

where $\mathbf{W}_0$ and $\mathbf{D}_0$ are normalized vorticity and rate-of-strain tensors for the pure shear velocity field $\mathbf{v}=(2y,0,0)$,

$$\mathbf{W}_0=\begin{pmatrix}0 & 1 & 0\\ -1 & 0 & 0\\ 0 & 0 & 0\end{pmatrix},\quad \mathbf{D}_0=\begin{pmatrix}0 & 1 & 0\\ 1 & 0 & 0\\ 0 & 0 & 0\end{pmatrix},\quad \mathbf{U}=\begin{pmatrix}\cos\theta & \sin\theta & 0\\ -\sin\theta & \cos\theta & 0\\ 0 & 0 & 1\end{pmatrix},$$

$$\cos 2\theta=\frac{b}{\sqrt{b^2+c^2}},\quad \sin 2\theta=-\frac{c}{\sqrt{b^2+c^2}},$$

$$b=ap+\chi H_1H_2,\quad c=av_{11}+\chi\frac{H_1^2-H_2^2}{2},\quad \lambda=\sqrt{b^2+c^2}. \tag{15}$$

In the new configurational coordinates $\mathbf{n}=\mathbf{U}\cdot\mathbf{m}$, the Smoluchowski equation takes the form

$$\frac{d\hat{f}}{dt}=\mathcal{R}_n\cdot[D_r(a)\tilde{f}\mathcal{R}_n\tilde{\mu}]-\mathcal{R}_n\cdot\left[\mathbf{n}\times\left(\dot{\mathbf{n}}-\frac{\chi H^2}{2}\mathbf{e}_3\mathbf{e}_3\cdot\mathbf{n}\right)\tilde{f}\right],$$

$$\dot{\mathbf{n}}=\tilde{\mathbf{W}}\cdot\mathbf{n}+\tilde{a}[\tilde{\mathbf{D}}\cdot\mathbf{n}-\tilde{\mathbf{D}}:\mathbf{nnn}], \tag{16}$$

where $\tilde{\mathbf{W}}=q\mathbf{W}_0$, $\tilde{\mathbf{D}}=q\mathbf{D}_0$, and $\tilde{a}=\lambda/q$.

This transformed system (16), by comparison with Eq. (3), corresponds to a simple shear flow with effective shear rate $2q$, a modified spheroidal shape parameter $\tilde{a}$, together with an imposed magnetic field in direction $\mathbf{e}_3$ normal to the shearing plane, and most importantly, the anisotropy $-(\chi/2)$ is opposite of the original one for the same material. *The response to arbitrary coupled coplanar flow and magnetic fields is now accessible by solution of the transformed or "reduced kinetic model" (16), which requires a simple shear flow code for LCPs with one more transverse field component with negative anisotropy*. One immediately accessible question is: how are the various time periodic and chaotic responses of nematic polymers in planar, shear-dominated linear flows [Faraoni *et al.* (1999); Grosso *et al.* (2001); Rienacker *et al.* (2002); Larson and Öttinger (1991); Forest and Wang (2003); Forest *et al.* (2004a, 2004b, 2004c, 2004d)] modified by a coplanar magnetic field as the field strength is varied?

Before answering this question, we complete the discussion on the remaining case where $q=0$, i.e., there is no rotational flow component and the system consists of excluded volume coupled with coplanar extensional flow and magnetic fields. Here, we can choose

$$\cos 2\theta=\frac{c}{\sqrt{b^2+c^2}},\quad \sin 2\theta=\frac{b}{\sqrt{b^2+c^2}} \tag{17}$$

so that the effective rate-of-strain tensor is diagonal $\lambda\mathbf{D}_1$, where

$$\mathbf{D}_1=\begin{pmatrix}1 & 0 & 0\\ 0 & -1 & 0\\ 0 & 0 & 0\end{pmatrix}. \tag{18}$$

Now, the corresponding flow is a planar extension or elongation

$$\mathbf{v}=\lambda(x,-y,0), \tag{19}$$

which is a potential flow with the corresponding normalized potential given by

$$V_e = -\frac{a\lambda}{2D_r}\mathbf{D}_1:\mathbf{mm}. \tag{20}$$

The coupled flow-magnetic interaction can be recast in terms of a total normalized potential given by

$$V = V_i(\mathbf{m}) - \frac{a\lambda kT}{2D_r}\mathbf{D}_1:\mathbf{mm} + \frac{\chi kT}{4D_r}H^2\mathbf{e}_3\mathbf{e}_3:\mathbf{mm}. \tag{21}$$

The Smoluchowski equation is then expressible in simplified form:

$$\frac{d}{dt}f = \mathcal{R}\cdot D_r\left(\mathcal{R}f + \frac{1}{kT}\mathcal{R}Vf\right). \tag{22}$$

The steady states are thus given by a Boltzmann distribution [Wang *et al.* (2005)]

$$f(\mathbf{m}) = \frac{1}{Z}e^{-V/kT}. \tag{23}$$

In steady state, the ensemble averaged torque vanishes

$$\langle \mathcal{R}V\rangle = 0. \tag{24}$$

This is equivalent to

$$\epsilon_{ijk}\left(\frac{a\lambda}{2D_r}\mathbf{D}_1 - \frac{\chi H^2}{4D_r}\mathbf{e}_3\mathbf{e}_3\right)_{il}\cdot \mathbf{M}_{lj} = 0, \tag{25}$$

where $\mathbf{M}=\langle\mathbf{mm}\rangle=\int_{\|\mathbf{m}\|=1}\mathbf{mm}f d\mathbf{m}$ is the second moment of $\mathbf{m}$ with respect to the PDF f. This in turn implies

$$M_{12} = M_{13} = M_{23} = 0 \tag{26}$$

if $a\lambda \neq -(\chi H^2/2)$. If $a\lambda=-(\chi H^2/2)$, $M_{12}=M_{23}=0$; if $a\lambda=\chi H^2/2$, $M_{12}=M_{13}=0$. In these latter cases, it can be shown $\mathbf{M}$ is diagonal as well. Thus, the principal axes of the rate-of-strain tensor coincide with those of the second moment tensor and both share the external field direction $\mathbf{e}_3$ as a principal axis. This result automatically implies all steady states have peak alignment either in the plane of the flow and magnetic field, or along the normal direction; that is, the anomalous pairs of "out of plane steady states" that exist in shear [Forest and Wang (2003)] cannot exist.

We return now to the general case with a rotational flow component. This generalized flow-magnetic field symmetry is inherited by any second moment tensor model that respects rotational invariance of the excluded volume potential. We shall illustrate the theoretical results above for a particular closure model of Doi-Hess theory that captures many qualitative features of the full kinetic model [Larson and Öttinger (1991); Forest and Wang (2003); Hess (1976); Rey (1995a); Rey (1995b)]. We denote $\mathbf{M}=\langle\mathbf{mm}\rangle$, $\mathbf{M}_4=\langle\mathbf{mmmm}\rangle$ as the second, fourth moments of the PDF, respectively, and use the Maier-Saupe excluded-volume potential [Doi and Edwards (1986)]

$$V_i = -\frac{3}{2}NkT\mathbf{M}:\mathbf{mm}. \tag{27}$$

It follows from Forest and Wang (2003) that

$$\frac{d}{dt}\tilde{\mathbf{M}} - \tilde{\mathbf{W}} \cdot \tilde{\mathbf{M}} + \tilde{\mathbf{M}} \cdot \mathbf{W} - \left[\left(\left(\tilde{a}\tilde{\mathbf{D}} - \frac{\chi}{2} H^2 \mathbf{e}_3\mathbf{e}_3 \right) \cdot \tilde{\mathbf{M}} \right) + \tilde{\mathbf{M}} \cdot \left(\tilde{a}\tilde{\mathbf{D}} - \frac{\chi}{2} H^2 \mathbf{e}_3\mathbf{e}_3 \right) \right]$$
$$= -2\left(\tilde{a}\tilde{\mathbf{D}} - \frac{\chi}{2} H^2 \mathbf{e}_3\mathbf{e}_3 \right):\tilde{\mathbf{M}}_4 - 6D_r[\tilde{\mathbf{M}} - \mathbf{I}/3 - n\tilde{\mathbf{M}} \cdot \tilde{\mathbf{M}} + N\tilde{\mathbf{M}}:\tilde{\mathbf{M}}_4], \tag{28}$$

where $\tilde{\mathbf{M}}_4 = \langle \mathbf{nnnn} \rangle$ and $\tilde{\mathbf{M}} = \langle \mathbf{nn} \rangle$. We note that $\tilde{a} = \lambda$ when $q=0$ and $\tilde{\mathbf{W}}=0$ (planar extension).

We approximate the fourth moment using a parametrized closure for any symmetric tensor $\mathbf{C}$:

$$\mathbf{C}:\tilde{\mathbf{M}}_4 = a_i \mathbf{C}:\tilde{\mathbf{M}}\tilde{\mathbf{M}} + \frac{(1-a_i)}{2}(\mathbf{C} \cdot \tilde{\mathbf{M}} + \tilde{\mathbf{M}} \cdot \mathbf{C}), \tag{29}$$

where $0 < a_i \leq 1$ in each application of the rule. The above system, after two applications of this rule, becomes

$$\frac{d}{dt}\tilde{\mathbf{M}} - \mathbf{W} \cdot \tilde{\mathbf{M}} + \tilde{\mathbf{M}} \cdot \mathbf{W} - a_2\left[\left(\left(\tilde{a}\tilde{\mathbf{D}} - \frac{\chi}{2} H^2 \mathbf{e}_3\mathbf{e}_3 \right) \cdot \tilde{\mathbf{M}} \right) + \tilde{\mathbf{M}} \cdot \left(\tilde{a}\tilde{\mathbf{D}} - \frac{\chi}{2} H^2 \mathbf{e}_3\mathbf{e}_3 \right) \right]$$
$$= -2a_2\left(\tilde{a}\tilde{\mathbf{D}} - \frac{\chi}{2} H^2 \mathbf{e}_3\mathbf{e}_3 \right):\tilde{\mathbf{M}}\tilde{\mathbf{M}} - 6D_r[\tilde{\mathbf{M}} - \mathbf{I}/3 - a_1 N\tilde{\mathbf{M}} \cdot \tilde{\mathbf{M}} + a_1 N\tilde{\mathbf{M}}:\tilde{\mathbf{M}}\tilde{\mathbf{M}}]. \tag{30}$$

We now select closure parameters to match features of the kinetic isotropic-nematic phase diagram without any external fields [Forest *et al.* (2004c, 2004d)]. The tensor model (30) has isotropic and nematic equilibria $\tilde{\mathbf{M}} = s_0(\mathbf{n}^*\mathbf{n}^* - (1/3)\mathbf{I}) + (1/3)\mathbf{I}$, where the order parameter s_0 is given by

$$s_0 = 0, \frac{1 \pm 3\sqrt{1 - 8(3a_1 N)}}{4} \tag{31}$$

and $\mathbf{n}^*$ is the uniaxial director (which is arbitrary). There are two critical concentrations, both fixed by a_1: the onset of nematic equilibria $N_c^{(1)} = 8/3a_1$ and the instability of the isotropic phase $N_c^{(2)} = 3/a_1$. We fix $a_1 = 3/5$, $N_c^{(2)} = 5$, which matches the result of kinetic theory exactly, and $N_c^{(1)} = 40/9 \approx 4.44$, which is very close to the kinetic theory value 4.49. The second closure parameter a_2 could be used to fit to another field-induced kinetic model bifurcation. For purposes here, we set $a_1 = 0.6$, $a_2 = 1$, which absorbs a_2 into the shape parameter $\tilde{a}$, and explore parametric behavior in the transformed (i.e., reduced) model to illustrate phenomena associated with coupled coplanar flow and magnetic fields.

We nondimensionalize the orientation tensor equation for $\tilde{\mathbf{M}}$ by the time scale set by rotary diffusivity $t_0 = 1/6D_r$. Then

$$\hat{q} = qt_0, \quad \hat{\lambda} = \lambda t_0, \quad \hat{\chi} = \chi H_0^2 t_0, \tag{32}$$

where H_0 is a characteristic field strength. We identify $\mathrm{Pe} = 2\hat{q}$ as the Peclet number in simple shear or $\mathrm{Pe} = \tilde{a}\lambda$ as the effective Peclet number in planar extension. For convenience, we hereafter drop the "hat" on all dimensionless parameters.

V. SIMPLE SHEAR FLOWS COUPLED WITH A TRANSVERSE MAGNETIC FIELD AND A NEGATIVE ANISOTROPY

We first study parametric behavior of the reduced model, consisting of simple shear coupled to a transverse magnetic field of variable strength. (Afterward, we will relate these phenomena to the original formulation of coupled, coplanar, magnetic, and linear flow fields.)

From the formula for the modified shape parameter

$$\tilde{a} = \frac{1}{q}\sqrt{\left[\frac{\chi}{2}(H_1^2 - H_2^2)\right]^2 + (ap + \chi H_1 H_2)^2} \tag{33}$$

we note that the magnetic field strength, material anisotropy, molecular geometry, and velocity components contribute to $\tilde{a}$. From previous studies, for sufficiently large stretching rates, the only stable orientational distributions exhibit steady alignment in the flow plane [Forest and Wang (2003); Forest *et al.* (2004d)]. This translates to a well-known experimental observation: a sufficiently strong magnetic field strength will overwhelm any linear flow field and induce a steady alignment of the nematic liquid.

On the other hand, if $\tilde{a}$ is not large enough to force a stable, steady, aligned orientational distribution, the pure shear dynamics will be modified by the transverse magnetic field $H^2\mathbf{e}_3$, and the negative anisotropy $-(\chi/2)$. We now explore this interaction, anticipating a "taming effect" of the magnetic field with respect to complex dynamic responses to shear dominated flow. By this we mean that the magnetic field should be capable of arresting the dynamics induced by shear, at some threshold field strength that is to be determined by this analysis.

We explore the impact of the transverse magnetic field with respect to three representative regimes of the effective Peclet number Pe. The three typical sheared responses we explore are two types of kayaking limit cycles and a chaotic orbit. We determine the phase transition sequence, or bifurcation diagram, as the magnetic field strength is increased from zero. In the following examples, we treat $\tilde{a}$ and $\tilde{\mathbf{H}}$ as independent parameters, and investigate how the variation in anisotropy and field strength $(\tilde{\mathbf{H}})$ affects the attractors of the model system at fixed values of $(\mathrm{Pe}, \tilde{a})$.

A. Regime 1: Magnetic field influence on kayaking orbits at small fixed Pe and fixed $\tilde{a}$

When the magnetic field strength is zero, the stable solution or attractor of Eq. (30) at selected parameter values, $\mathrm{Pe}=1.5$, $\tilde{a}=0.8$, $N=6$, is a so-called "kayaking orbit," a name coined by Larson and Öttinger (1991), and labeled "K" in our figures. This limit cycle response to shear corresponds to a peak axis of orientation rotating around the flow vorticity axis. When the magnetic field (along the vorticity axis of symmetry of the kayaking orbit) is turned on parametrically, the effect of negative magnetic anisotropy is to push the oscillations of the peak axis away from the vorticity axis toward the flow-flow gradient plane. As the magnetic field strength is increased, there is an out-of-plane to in-plane transition to the classical tumbling orbit (with peak director rotating continuously in the flow plane). This transition among periodic limit cycles is through a period-halving bifurcation, depicted in Fig. 1, so that the tumbling orbit is twice as fast as the kayaking limit cycle. The transverse magnetic field and negative magnetic anisotropy thus forces out-of-plane kayaking orbits in pure shear onto in-plane tumbling orbits. (The negative anisotropy has a repulsive effect, pushing the limit cycle into the plane normal to the magnetic field direction.)

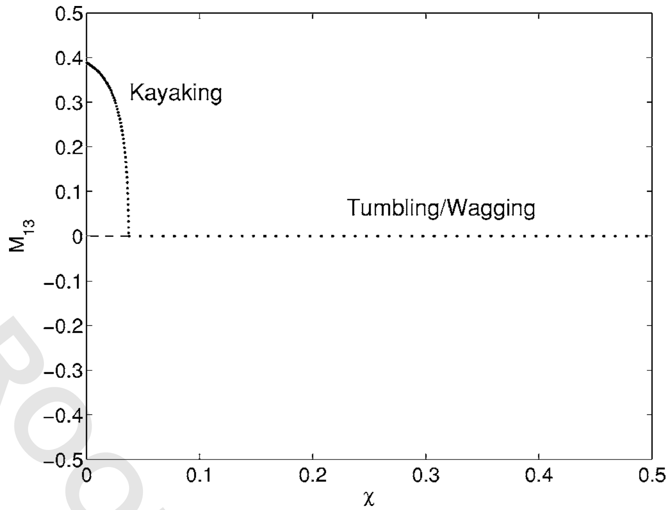

FIG. 1. Out-of-plane orientation tensor component M_{13}, time averaged, as a function of magnetic anisotropy χ at parameter values Pe=1.5, $\tilde{a}$=0.8 and N=6. As χ increases, the out-of-plane kayaking orbit collapses onto an in-plane, tumbling orbit. The dotted curves indicate stability and all other curves correspond to unstable model solutions.

B. Regime 2: Magnetic field influence on chaotic sheared dynamics at intermediate Pe and fixed $\tilde{a}$

At zero magnetic field strength, we fix the flow and aspect ratio parameters so that the attractor is chaotic [Grosso *et al.* (2001); Forest and Wang (2003)]. We then adiabatically raise the field strength and observe the attractor transitions, anticipating steady alignment at very strong field strength. Figure 2 depicts a representative bifurcation diagram for this

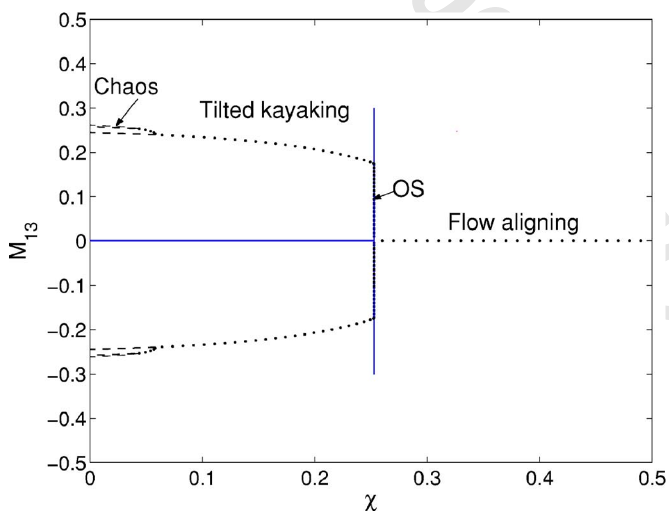

FIG. 2. M_{13}, time averaged, as a function of χ at parameter values Pe=3.1, $\tilde{a}$=0.8 and N=6. The shear response is chaotic for zero anisotropy χ=0. As χ increases, the chaotic attractor spawns a pair of tilted kayaking orbits through a sequence of period-halving bifurcations, then at higher field strengths the limit cycle orbits are arrested, resulting in steady alignment. The dotted curves are stable solutions while the others are unstable model solutions.

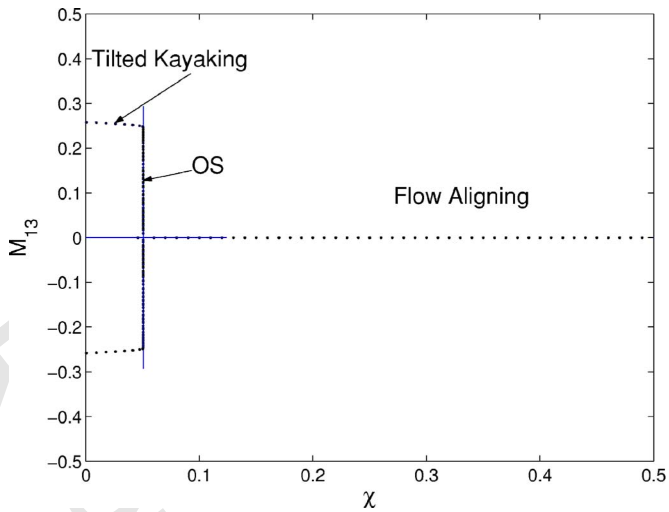

FIG. 3. M_{13}, time averaged, as a function of χ at parameter values Pe=3.6, $\tilde{a}$=0.8 and N=6. In this parameter regime, the bistable attractors are tilted kayaking orbits in pure shear (χ=0). As χ increases, the out-of-plane tilted kayaking orbits are arrested, leading to in-plane, steady distributions.

parameter regime, where the seemingly vertical line represents the arc of out-of-plane steady state pairs that connects the out-of-plane tilted kayaking states to flow-aligned steady states [Forest and Wang (2003)]. Alternatively, one can view this result from a steady aligned magnetic field strength, and explore the transition sequence as the magnetic field is slowly turned off: the prediction is a unique steady state alignment along the magnetic field axis at high field strengths, giving way to a pair of out-of-plane steady states (labeled OS), then Hopf and periodic-doubling bifurcations to chaos for sufficiently weak magnetic field strength. Thus, the model predicts the transition between shear-dominated rheochaos and magnetic-field-dominated steady state alignment.

C. Regime 3: Magnetic field influence on kayaking orbits at intermediate Pe and fixed $\tilde{a}$

We fix the normalized shear rate so that the stable attractor consists of pairs of so-called "tilted kayaking orbits" at zero magnetic field strength. We find a stable steady orientational distribution exists for sufficiently strong magnetic field. The transition sequence versus magnetic field strength is depicted in Fig. 3, consisting of an unsteady-to-steady transition (a supercritical Hopf bifurcation) from tilted kayaking orbits to out-of-plane steady states, followed by a sharp in-plane transition.

In summary, these three illustrations show that an imposed transverse magnetic field of sufficient strength and negative anisotropy arrests any time-dependent, shear-induced orbits, whether they are periodic or chaotic. A more subtle phenomenon occurs for intermediate magnetic field strengths applied to sheared kayaking orbits: the out-of-plane kayaking orbit is drawn into a tumbling orbit confined to the shear plane. These solutions of the reduced model are now translated back to the original model.

VI. MAPPING BETWEEN SOLUTIONS OF THE REDUCED MODEL AND THE FULLY COUPLED SYSTEM

In the previous section, we conducted a parametric study of the reduced model for LCPs: shear flow with an imposed magnetic field in the normal direction to the shearing plane and a negative magnetic anisotropy of the macromolecules. The outcomes of particular physical experiments are thereby predicted; however, the point of the theoretical results presented here is that these exact outcomes, up to an orthogonal transformation of coordinates, are shared by a large number of additional physical experiments. We amplify these results in two directions, using the solutions presented above: mapping from fixed parameters in the reduced model back to the original formulation of coplanar magnetic and linear flow fields; and, starting from a coplanar flow and magnetic field problem, projecting by the symmetry principle onto the reduced model.

We first establish the family of planar linear flows and coplanar magnetic field that correspond to any given reduced shear flow solution. That is, we begin from a fixed parameter set $(\mathrm{Pe},\tilde{a},H^2)$ of the reduced problem where we fix the anisotropy parameter χ_a, and determine which parameter set(s) $(v_{11},v_{12},v_{21},H_1,H_2,a,\chi)$ in the original physical model share the same PDF or second-moment tensor, up to an orthogonal transformation, by virtue of the symmetry. Recall the classical flow-magnetic analogy is a one-to-one correspondence; by contrast, as shown in [Forest *et al.* (2004a); Forest *et al.* (2004b)], the flow-molecular geometry symmetry exhibits a two-parameter degeneracy. Here, for strongly coupled magnetic and flow fields, there is a three-parameter degeneracy. Namely, *each solution of the reduced model problem corresponds to a three-parameter family of linear planar flows of LCPs with coplanar magnetic fields*.

Specifically, we first construct $\mathbf{v}=(v_{11}x+v_{12}y,v_{21}x-v_{11}y,0)$, $\mathbf{H}=(H_1,H_2,0)$, and a from given $\mathrm{Pe},\tilde{a}$ and H^2 through

$$\tilde{a}=\frac{2}{v_{12}-v_{21}}\sqrt{\left(\frac{a}{2}(v_{12}+v_{21})+\chi H_1H_2\right)^2+\left[av_{11}+\frac{\chi}{2}(H_1^2-H_2^2)\right]^2}$$

$$\mathrm{Pe}=(v_{12}-v_{21}),$$

$$H^2=H_1^2+H_2^2. \tag{34}$$

This is a 6-to-3 mapping between parameters of the original model, $(v_{11},v_{12},v_{22},H_1,H_2,a)$, and those of the reduced model, $(\mathrm{Pe},\tilde{a},H^2)$.

We next illustrate how a physically meaningful four-mill flow [Bentley and Leal (1986); Bird *et al.* (1987); Fuller and Leal (1981)] for LCPs of the geometry parameter $a=0.8$

$$\mathbf{v}=G[(1+\gamma)x+(1-\gamma)y,-(1-\gamma)x-(1+\gamma)y,0]^T,$$

$$v_{12}=G(1-\gamma),\quad v_{11}=G(1+\gamma),\quad v_{21}=-G(1-\gamma) \tag{35}$$

relates to the reduced simple shear model. Without loss of generality, we set $H^2=1$ and parametrize the planar magnetic field by

$$H_1=\cos\phi,\quad H_2=\sin\phi. \tag{36}$$

The 6–3 mapping reduces to a 3–2 mapping between the parameters in the original model: (G,γ,ϕ) and the ones in the reduced model: $(\mathrm{Pe},\tilde{a})$ according to Eq. (34), which in these new parameters become:

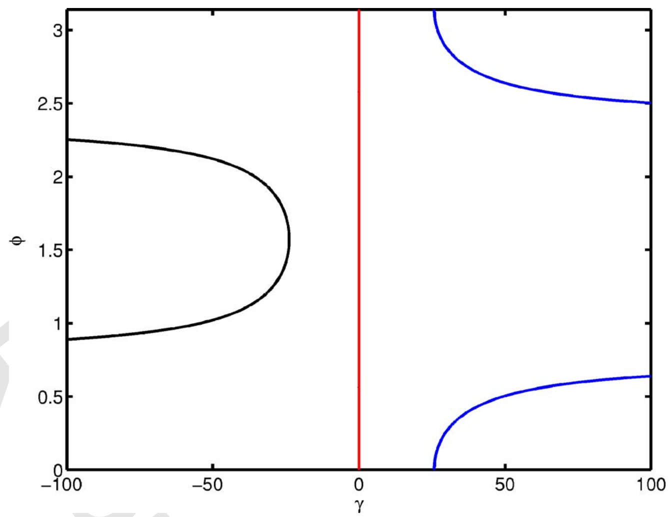

FIG. 4. The shear component γ in four-roll mill flows vs magnetic field angle ϕ diagram for molecular aspect ratio $r=3$ ($a=0.8$), which can be mapped to the reduced shear flow model with Pe=3.1, $\tilde{a}=0.8$. $G=\mathrm{Pe}/2(1-\gamma)$.

$$(\tilde{a}\mathrm{Pe})^2 = (\chi \sin 2\phi)^2 + \left(\frac{a\mathrm{Pe}(1+\gamma)}{1-\gamma} + \chi \cos 2\phi\right)^2,$$

$$\mathrm{Pe} = 2G(1-\gamma). \quad (37)$$

At this stage, we have the freedom to specify any four-roll mill flow (by fixing G,γ), and any direction ϕ of the coplanar magnetic field. Recall at the outset, the symmetry is valid for any strength of the excluded volume interaction potential and for any magnetic susceptibility parameter χ_a. We will assert a potential strength $N=6$ and modified magnetic susceptibility $\chi=0.2$ in all illustration below.

We exercise this freedom now, specifying the three remaining parameters: the four-roll mill flow type, $G=1.6125$, $\gamma=0.03876$, and the coplanar magnetic field direction $\phi=\pi/2$. This unique experimental condition now maps, by relations (37), onto the reduced model with dictated parameters (Pe=3.1, $\tilde{a}=0.8$). We now refer back to Fig. 2, where this reduced model has already been solved in the course of our parametric study (by design, of course). The bistable responses are a pair of tilted kayaking orbits! Thus the experiment of interest has the same bistable, periodic limit cycle attractors, where the axis of symmetry of the limit cycles is simply rotated by the rotation matrix U defined earlier in Eq. (15).

Conversely, relations (37) with dictated parameters (Pe=3.1, $\tilde{a}=0.8$) do not uniquely specify G,γ,ϕ at the values 1.6125, 0.03876, $\pi/2$; there is a one parameter family of G,γ,ϕ for reduced model parameters Pe=3.1, $\tilde{a}=0.8$. Figure 4 depicts this one-parameter family of values parametrized by the shear component γ, depicting the angle of the coplanar magnetic field ϕ for allowable γ, while the value of G versus γ is prescribed as $G=\mathrm{Pe}/2(1-\gamma)$.

If we relax the restrictions outlined above in order to focus on a particular class of four-roll mill flows, Eq. (34) gives more general linear planar flows of modified geometry parameter fluids and coplanar magnetic fields that map to the same reduced model parameters. In general, there is a full three-parameter family of original model parameters that has the exact same reduced model parameter values Pe=3.1, $\tilde{a}$=0.8, and therefore all share this bistable pair of tilted kayaking orbits. This fact is furthermore true for all values of Pe, $\tilde{a}$, so that the bifurcation diagrams illustrated in the previous section, and phenomena associated with magnetic field strength variations, can each be traced back to experimental conditions as described in this example.

VII. PLANAR EXTENSIONAL FLOWS COUPLED WITH A COPLANAR MAGNETIC FIELD

Finally, we study the reduced model for the limiting case of a planar extensional flow (irrotational flow) coupled with a coplanar magnetic field. The corresponding reduced model is easily seen to be a planar extensional flow subject to a magnetic field in the direction normal to the flow plane with a negative anisotropy. The combined effects of planar extension and the perpendicular magnetic field are seen, by the flow-magnetic field symmetry, to correspond to a three-dimensional triaxial elongational flow! We find that the effective rate-of-strain tensor, in the frame of the principal axes or directors of the second moment **M**, is given by:

$$\mathbf{D}_3 = \mathrm{diag}\left(a\lambda + \frac{\chi}{6}, -a\lambda + \frac{\chi}{6}, -\frac{\chi}{3}\right). \tag{38}$$

The stretch or compression rate is given by the diagonal entries, which are generically, distinct.

Our previous studies on uniaxial and biaxial elongation indicate that the kinetic model and its mesoscopic closures do not support any time-periodic stable solutions, either in-plane or out-of-plane in the strong flow field [Wang (1997); Forest *et al.* (2004a); Forest *et al.* (2004b); Wang *et al.* (2005)]. With this triaxial elongational flow of the target model, there is no reason to expect stable periodic solutions either. We thus write the orientation tensor in its biaxial representation parametrized by an in-plane angle variable $\xi(t)$

$$\mathbf{M} = s(t)\left(\mathbf{nn} - \frac{\mathbf{I}}{3}\right) + \beta(t)\left(\mathbf{n}^{\perp}\mathbf{n}^{\perp} - \frac{\mathbf{I}}{3}\right) + \frac{\mathbf{I}}{3}, \tag{39}$$

where s and β are the order parameters and the two in-plane major directors:

$$\mathbf{n} = (\cos\xi(t), \sin\xi(t), 0)^T, \quad \mathbf{n}^{\perp} = (-\sin\xi(t), \cos\xi(t), 0)^T. \tag{40}$$

The third major director is perpetually fixed in the normal direction of the plane. The governing equation for the orientation tensor (30) reduces to a set of equations for the order parameters and the angle variable:

$$\frac{ds}{dt} = -U(s) + \frac{2Ns\beta}{3}(1+\beta-s) - \frac{\chi H^2}{2}(1+s)(s+\beta-1) - \mathrm{Pe}\cos 2\xi\left(s^2 - 2s\beta - \frac{4}{3}s + \frac{2\beta}{3} - \frac{2}{3}\right),$$

$$\frac{d\beta}{dt} = -U(\beta) + \frac{2Ns\beta}{3}(1+s-\beta) - \frac{\chi H^2}{2}(1+\beta)(s+\beta-1) + \mathrm{Pe}\cos 2\xi\left(\beta^2 - 2s\beta + \frac{2}{3}s - \frac{4\beta}{3} - \frac{2}{3}\right),$$

$$\frac{d\xi}{dt} = \frac{\text{Pe}\sin 2\xi(s+\beta+2)}{3(\beta-s)}, \tag{41}$$

where $U(s)=s[1-(N/3)(1-s)(2s+1)]$ and $\text{Pe}=a\lambda$ is an effective Peclet number with the geometry parameter a included.

The steady states of the third equation in Eq. (41) lead directly to $\xi=0$, $\pi/2$, indicating the two in-plane directors must be coaxial with principal axes of the rate-of-strain tensor. When the directors are aligned with principal axes of the rate-of-strain tensor, the order parameter dynamics are limited to isolated attractors or steady states that exhibit biaxiality. In steady states, the system of governing equations preserves the following symmetry properties for all solutions:

- if $(s,\beta,\xi=0)$ is a solution, so is $(\beta,s,\xi=\pi/2)$;
- if (s,β,ξ,Pe) is a solution, so is $(\beta,s,\xi,-\text{Pe})$;
- when $\text{Pe}=0$, (s,β) is a solution, so is (β,s) since the flow is biaxial elongation with the axis of symmetry in the normal direction of the plane.

According to the symmetry properties, the solutions can be obtained with $\xi=\pi/2$ should we find the solutions for $\xi=0$. Similarly, we obtain the steady state solutions for planar extension with $-\text{Pe}$ should we know the solutions for Pe. After a lengthy simplification, we deduce that the steady state condition for the order parameter s is a seventh-order polynomial equation given in the Appendix. The corresponding solutions for β are then obtained using the same equation for s while replacing Pe by $-\text{Pe}$ following the symmetry properties on Pe outlined above. This symmetry yields nontrivial numerical simplification in calculating the steady states.

In order to investigate the impact of the transversely imposed magnetic field on planar extension of flowing LCPs with a negative anisotropy, we first benchmark the planar extension flow behavior free of the magnetic field. Figure 5 depicts the phase diagram for the order parameters (s,β) as functions of N with respect to $\text{Pe}=0,0.01,0.1,0.4$; it shows the gradual departure from uniaxiality ($s=0$, $\beta=0$, or $s=\beta$) in the order parameters as $|\text{Pe}|$ increases. Except for a small interval of bistability in Pe, the steady state with its major director in the stretching direction (the x axis in posited planar extension $\mathbf{v}=\text{Pe}(x,-y,0)$ becomes the only stable steady state. Whereas in uniaxial elongation the stable solution is uniaxial in elongation and biaxial in compression at high concentration [Wang (1997)]. We notice that the biaxiality along this solution branch is extremely weak; the order parameter solution behavior is quite similar to the elongational flow in three dimensions [Wang (1997)].

We denote the eigenvalues of the second moment tensor $\mathbf{M}$ by d_i, $i=1,2,3$, which represent the degrees of orientation with respect to the principal axes (eigenvector directions) [Forest *et al.* (1997)]. Suppose d_1 has corresponding eigenvector $\mathbf{n}$, d_2 with $\mathbf{n}^{\perp}$. It follows from (39)

$$s=d_1-d_3, \quad \beta=d_2-d_3. \tag{42}$$

For the stable branches in Fig. 5, we notice that the order parameters $s>0$, $\beta<0$. This shows that the degree of orientation along the stable biaxial branch satisfies the following order:

$$d_2<d_3<d_1. \tag{43}$$

Thus, this stable biaxial phase possesses the highest degree of orientation in the principal stretching direction of the flow $\mathbf{n}$, *followed next by the neutral direction, and is least oriented in the compression direction.*

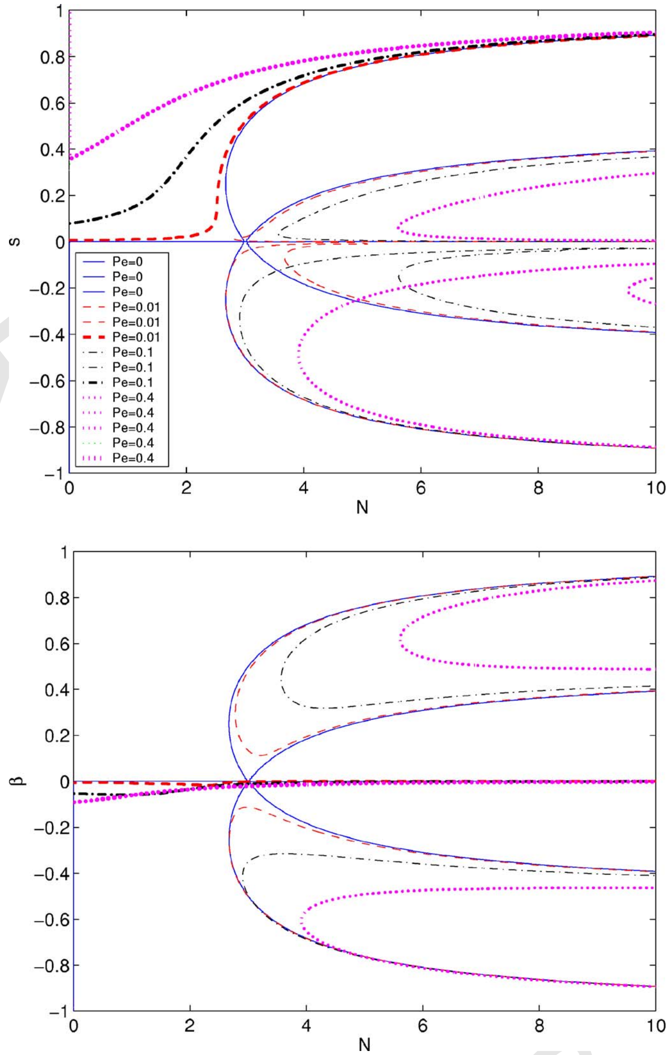

FIG. 5. The phase bifurcation diagram for planar extension flows absent of the external field at Pe $=0, 0.01, 0.1, 1$, respectively. The stable branch corresponding to nonzero Pe is given by thick curves.

We next consider the impact of the additional magnetic field imposed transverse to the flow plane on materials with a negative anisotropy. We illustrate the results on steady states with Pe$=0.1$ to contrast with the results in Fig. 5.

Figure 6 depicts the steady states as functions of the dimensionless concentration N with respect to $\chi=0,1,2,10$, respectively. The impact of the magnetic field is quantitative only. Now, the stretching rate is increased by $\chi/6$ in the direction of $\mathbf{n}$, the compression rate is decreased by the same amount in the direction of $\mathbf{n}^{\perp}$, and the compression rate is increased by $\chi/3$ in the perpendicular direction. This impacts the order parameter behavior by increasing the degree of orientation in the direction of $\mathbf{n}$, decreasing the degree of orientation in the normal direction of the plane while increasing the degree of orientation in the direction of $\mathbf{n}^{\perp}$. This translates into increased order in s and β simultaneously. For $\chi=1$, 5, 10, the effective generalized triaxial elongation stretches in the plane and compresses in its perpendicular direction. In these cases, the degree of orien-

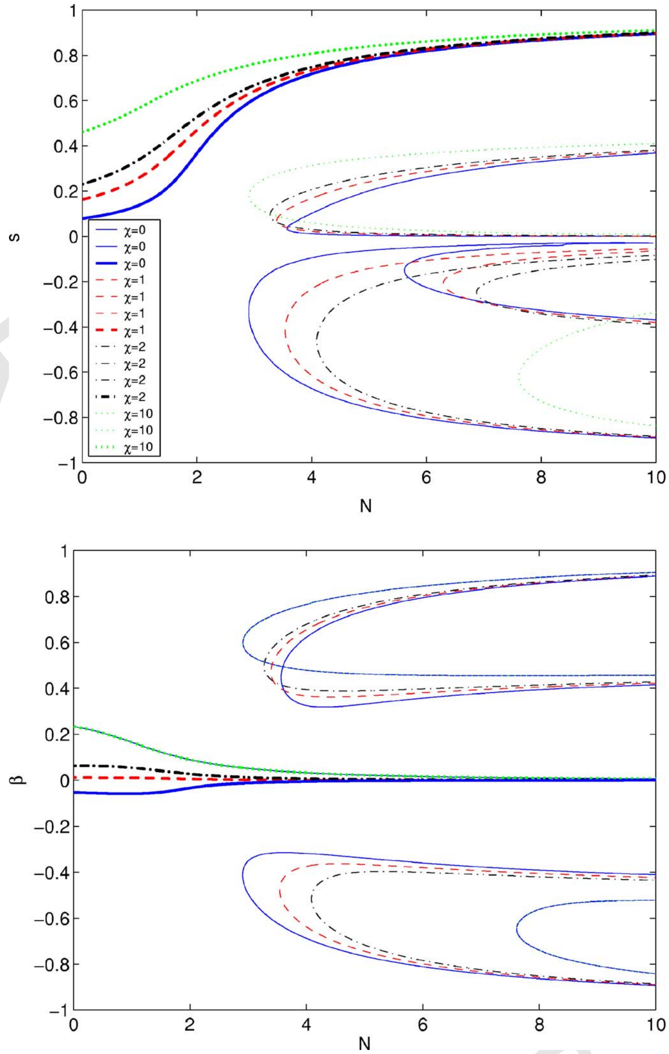

FIG. 6. The phase bifurcation diagram for planar extension flows subject to a transverse magnetic field with fixed weak extension rate Pe=0.1, and variable (negative) magnetic anisotropy $\chi = 0, 1, 2, 10$, respectively. The thick curves depict stable solution branches of the model.

tation in $\mathbf{n}^{\perp}$ is higher than that in the transverse direction, reflected in a positive β. By increasing the strength of the magnetic field or the magnitude of the anisotropy, this trend continues.

Finally, we examine the impact of the Peclet number (normalized extension rate) on steady states in the presence of the transversely imposed external field. Figure 7 depicts the solution for $\chi = 1$ at $\mathrm{Pe} = 0, 0.01, 0.1, 0.4$, respectively. At Pe=0, the solution of s and that of β is identical according to the symmetry. When Pe increases, again the stretching/compression rate provides a good diagnostic tool. The stretching rate in $\mathbf{n}$ increases and that in $\mathbf{n}^{\perp}$ decreases while the compression rate in the normal direction is held constant. The noticeable feature is that the stable order parameter β decays from a positive value

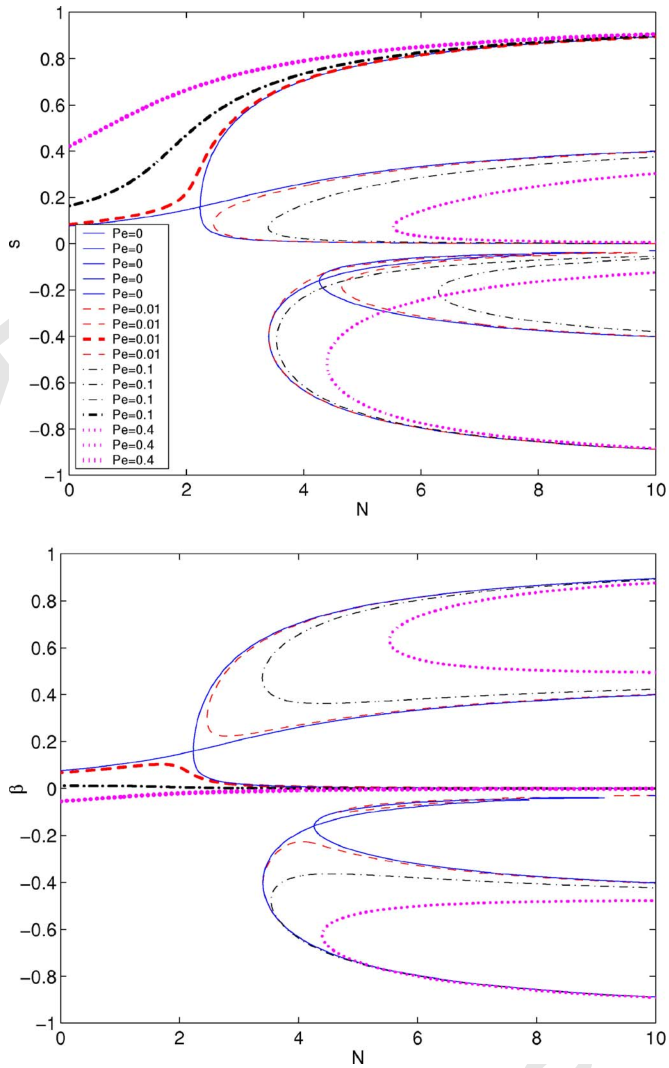

FIG. 7. The phase bifurcation diagram for planar extension flows subject to a transverse magnetic field with negative anisotropy $\chi=1$, vs normalized extension rate $\mathrm{Pe}=0, 0.01, 0.1, 0.4$, respectively. The thick curves depict stable solution branches.

at $\mathrm{Pe}=0$ to a negative one as Pe increases while s maintains positive. This indicates the degree of orientation in $\mathbf{n}^{\perp}$ decays relative to that in the normal direction as the stretching rate in that direction decreases from positive to negative.

In summary, the stable steady states exhibit weak biaxiality with the degree of orientation correlating well with the stretching rate of the triaxial elongation. A positive stretching rate aligns the rod ensemble along the flow principal axis, while a compression rate decreases alignment in that direction. These results are as expected on physical grounds; the gain, however, is that they are quantitative and have potential to be combined with experiments and material properties.

VIII. CONCLUSION

We have developed a generalized symmetry, extending the classical analogy between extensional flows and magnetic fields applied to liquid crystals (LCs). We consider the Doi-Hess theory of liquid crystal polymers (LCPs), where an excluded volume potential and the isotropic-nematic phase transition are leading order considerations. We then generalize the classical symmetry in two ways: from LCs to LCPs; and from a trade-off of flow and magnetic field to the strong coupling between excluded volume interactions and coplanar linear flow and magnetic fields. This generalized symmetry is more than a simple parameter trade-off (extension rate for magnetic field strength); rather, the six-parameter Smoluchowski equation or second-moment tensor model is transformed to a reduced model with only three flow-magnetic field parameters, making possible the exploration of the nonlinear interactions among three coupled fields. This symmetry-based model reduction generalizes previous results of the authors [Forest *et al.* (2004a)] to include a magnetic field coupling. The reduced model derived herein consists of an excluded volume potential and simple shear coupled with an imposed magnetic field in the flow vorticity direction, where the LCP has a negative magnetic anisotropy and a modified molecular geometry parameter. Shear-free planar extensional flows of LCPs with a coplanar magnetic field obey an even simpler reduced problem, consisting of an effective triaxial elongational flow. These reduced models are then amenable to existing numerical codes for simple shear or extensional flow of LCPs with a minor extension. We apply these results to predict LCP response diagrams in the presence of coupled coplanar linear flows and magnetic fields, restricting to second-moment models. The introduction of a magnetic field arrests the complex dynamics of sheared LCPs, as expected, yet we predict a sequence of phase transitions versus magnetic field strength. We also model a four-roll mill experiment with a coplanar magnetic field, illustrating the attractor transitions due to increased magnetic field strength, when the imposed flow is a linear combination of shear and extension. The results naturally extend to the coplanar, time-dependent, imposed magnetic field like rotating magnetic field.

ACKNOWLEDGMENTS

The authors acknowledge financial support from AFOSR grant Nos. FA9550-05-1-0025, FA9550-06-1-0063, NSF Grant Nos. DMS 0604891, 0604912, 0605029, 0626180, NASA URETI BIMat Award No. NCC-1-02037, and the Army Research Office.

APPENDIX: THE GOVERNING EQUATION FOR THE ORDER PARAMETER *s*

The governing equation for the order parameter s, which is also the governing equation for β should μ is replaced by $-\mu$, where $\mu=\mathrm{Pe}/a$.

$$
\begin{aligned}
&96x^7N^4-64a^3\mu^3+(480aN^3\mu+120N^3\chi)x^6-48a^2\chi\mu^2+(576a^2N^2\mu^2+144aN^3\mu\\
&+432aN^2\chi\mu-120N^4-12N^3\chi+48N^2\chi^2+288N^3)x^5-12a\chi^2\mu+(-384a^3N\mu^3\\
&+576a^2N^2\mu^2+288a^2N\chi\mu^2-576aN^3\mu+96aN^2\chi\mu+120aN\chi^2\mu+912aN^2\mu-144N^3\chi\\
&-12N^2\chi^2+6N\chi^3+228N^2\chi)x^4+(-768a^4\mu^4+576a^3N\mu^3-192a^3\chi\mu^3-672a^2N^2\mu^2\\
&+240a^2N\chi\mu^2+48a^2\chi^2\mu^2+480a^2N\mu^2-144aN^3\mu-480aN^2\chi\mu+12aN\chi^2\mu+12a\chi^3\mu\\
&+144aN^2\mu+432aN\chi\mu+24N^4+12N^3\chi-54N^2\chi^2-3N\chi^3-144N^3-12N^2\chi+46N\chi^2\\
&+216N^2)x^3-\chi^3+(384a^3N\mu^3-384a^3\mu^3-576a^2N^2\mu^2-288a^2N\chi\mu^2+192a^2N\mu^2
\end{aligned}
$$

$$+96a^2\chi\mu^2+96aN^3\mu-96aN^2\chi\mu-120aN\chi^2\mu-384aN^2\mu+32aN\chi\mu+56a\chi^2\mu+24N^3\chi$$
$$+12N^2\chi^2-6N\chi^3+288aN\mu-96N^2\chi-4N\chi^2+2\chi^3+72N\chi)x^2+(768a^4\mu^4-576a^3N\mu^3$$
$$+192a^3\chi\mu^3-192a^3\mu^3+96a^2N^2\mu^2-240a^2N\chi\mu^2-48a^2\chi^2\mu^2-224a^2N\mu^2-80a^2\chi\mu^2$$
$$+48aN^2\chi\mu-12aN\chi^2\mu-12a\chi^3\mu+96a^2\mu^2-112aN\chi\mu-4a\chi^2\mu+6N^2\chi^2+3N\chi^3$$
$$+48a\chi\mu-14N\chi^2+\chi^3+6\chi^2)x \qquad (44)$$

References

Bhandar, A. S., and J. M. Wiest, "Mesoscale constitutive modeling of magnetic dispersions," J. Colloid Interface Sci. **257**, 371–382 (2003).

Bentley, B. J., and L. G. Leal, "A computer controlled four-roll mill for investigation of particle and rope dynamics in two-dimensional linear shear flows," J. Fluid Mech. **167**, 219–240 (1986).

Bird, B. R., R. C. Armstrong, and O. Hassager, *Dynamics of Polymeric Liquids* (Wiley, New York, 1987), Vol. 1.

Chandrasekhar, S., *Liquid Crystals* (Cambridge University Press, London, 1992).

Constantin, P., and J. Vukadinovic, "Note on the number of steady states for a two-dimensional Smoluchowski equation," Nonlinearity **18**, 441–443 (2005).

Doi, M., and S. F. Edwards, *The Theory of Polymer Dynamics* (Clarendon, Oxford, 1986).

deGennes, P. G., and J. Prost, *The Physics of Liquid Crystals* (Oxford University Press, New York, 1993).

Faraoni, V., M. Grosso, S. Crescitelli, and P. L. Maffetone, "The rigid-rod model for nematic polymers: An analysis of the shear flow problem," J. Rheol. **43**, 829–843 (1999).

Feng, J., and L. G. Leal, "Numerical simulation of the flow of dilute polymer solutions in a four-roll mill," J. Non-Newtonian Fluid Mech. **72**, 187–218 (1997).

Forest, M. G., Q. Wang, and S. E. Bechtel, "1 dimensional isothermal spinning models for liquid crystalline polymer fibers," J. Rheol. **41**, 821–850 (1997).

Forest, M. G., Q. Wang, and H. Zhou, "Homogeneous pattern selection and director instabilities of nematic liquid crystal polymers induced by elongational flows," Phys. Fluids **12**, 490–498 (2000).

Forest, M. G., Q. Wang, and H. Zhou, "On the flow-phase diagram for discotic liquid crystals in uniaxial extension and compression," Liq. Cryst. **5**, 717–721 (2000).

Forest, M. G., and Q. Wang, "Monodomain response of finite-aspect-ratio macromolecules in shear and related linear flows," Rheol. Acta **42**, 20–46 (2003).

Forest, M. G., Q. Wang, R. Zhou, and E. Choate, "Monodomain response of arbitrary aspect ratio nematic polymers in general linear planar flows," J. Non-Newtonian Fluid Mech. **118**, 17–31 (2004a).

Forest, M. G., R. Zhou, and Q. Wang, "Chaotic boundaries of nematic polymers in mixed shear and extensional flows," Phys. Rev. Lett. **93**, 088301 (2004b).

Forest, M. G., Q. Wang, and R. Zhou, "The weak shear phase diagram for nematic polymers," Rheol. Acta **43**, 17–37 (2004c).

Forest, M. G., Q. Wang, and R. Zhou, "The flow-phase diagram of Doi-Hess theory for sheared nematic polymers II: Finite shear rates," Rheol. Acta **44**, 80–93 (2004d).

Forest, M. G., S. Sircar, Q. Wang, and R. Zhou, "Monodomain dynamics for rigid rod and platelet suspensions in strongly coupled coplanar linear flow and magnetic fields: Kinetic simulations," Phys. Fluids **18**, 103102 (2006).

Fuller, G. G., L. G. Leal, "Flow birefringence of concentrated polymer solutions in two-dimensional flows," J. Polym. Sci., Polym. Phys. Ed. **19**, 557–587 (1981).

Gopinath, A., L. Mahadevan, and R. C. Armstrong, "Transitions to nematic states in homogeneous suspensions of high aspect ratio magnetic rods," Phys. Fluids **18**, 028102 (2006).

Grosso, M., R. Keunings, S. Crescitelli, and P. L. Maffetone, "Prediction of chaotic dynamics of sheared liquid creystalline polymers," Phys. Rev. Lett. **86**, 3184–3187 (2001).

Hess, S., "Fokker-Planck-equation approach to flow alignment in liquid crystals," Z. Naturforsch. A **31a**, 1034–1037 (1976).

Isihara, A., "The theory of anisotropic colloidal solutions," J. Chem. Phys. **19**, 1142–1147 (1951).

Jeffery, G. B., "The motion of ellipsoidal particles immersed in a viscous fluid," Proc. R. Soc. London, Ser. A **102**, 161–179 (1922).

Kuzuu, N., and M. Doi, "Constitutive equations for nematic liquid crystals under weak velocity gradients derived from a molecular kinetic equation," J. Phys. Soc. Jpn. **52**, 3486–3494 (1983).

Larson, R. G., and H. C. Ottinger, "Effect of molecular elasticity on out-of-plane orientations in shearing flows of liquid crystalline polymers," Macromolecules **24**, 6270–6282 (1991).

Onsager, L., "The effects of shape on the interaction of colloidal particles," Ann. N.Y. Acad. Sci. **51**, 627–659 (1949).

Rey, A., "Bifurcational analysis of the isotropic-nematic phase transition of rigid rod polymers subjected to biaxial stretching flow," Macromol. Theory Simul. **4**, 857–872 (1995).

Rey, A., "Bifurcational analysis of the isotropic-discotic nematic phase transition in the presence of extensional flow," Liq. Cryst. **19**, 325–331 (1995b).

Rienacker, G., M. Kroger, and S. Hess, "Chaotic and regular shear-induced orientation dynamics of nematic liquid crystals," Physica A **315**, 537–568 (2002).

Wang, Q., "Comparative studies on closure approximations in flows of liquid crystal polymers. I Elongational flows," J. Non-Newtonian Fluid Mech. **72**, 141–162 (1997).

Wang, Q., "A hydrodynamic theory of nematic liquid crystalline polymers of different configurations," J. Chem. Phys. **116**, 9120–9136 (2002).

Wang, Q., S. Sircar, and H. Zhou, "Steady state solutions of the Smoluchowski equation for nematic polymers under imposed fields," Commun. Math. Sci. **4**, 605–620 (2005).

PROOF COPY 006701JOR